Non-cytotoxic Silver Nanoparticle-Polysaccharide Nanocomposites with Antimicrobial Activity

ARTICLE *in* BIOMACROMOLECULES · MAY 2009

Impact Factor: 5.75 · DOI: 10.1021/bm900039x · Source: PubMed

Non-cytotoxic Silver Nanoparticle-Polysaccharide Nanocomposites with Antimicrobial Activity

Andrea Travan,* Chiara Pelillo, Ivan Donati, Eleonora Marsich, Monica Benincasa, Tommaso Scarpa, Sabrina Semeraro, Gianluca Turco, Renato Gennaro, and Sergio Paoletti

Department of Life Sciences, University of Trieste, Via Giorgieri 1, Trieste I-34127, Italy

Received January 9, 2009; Revised Manuscript Received April 7, 2009

In this work we study (i) the formation and stabilization of silver nanoparticles in a bioactive chitosan-derived polysaccharide solution, (ii) the antimicrobial properties, either in solution or in 3D hydrogel structures, obtained by mixtures with the polysaccharide alginate, and (iii) the cytotoxicity of the latter nanocomposite materials on different eukaryotic cell lines. Antimicrobial results show that these nanocomposite systems display a very effective bactericidal activity toward both Gram+ and Gram− bacteria. However, the hydrogel does not show any cytotoxic effect toward three different eukaryotic cell lines. This is due to the fact that the nanoparticles, immobilized in the gel matrix, can exert their antimicrobial activity by simple contact with the bacterial membrane, while they can not be uptaken and internalized by eukaryotic cells. This novel finding could advantageously contribute to responding to the growing concerns on the toxicity of nanoparticles and facilitate the use of silver−biopolymer composites in the preparation of biomaterials.

1. Introduction

Since ancient times, silver has been extensively used to control infections. At present, silver as an antimicrobial agent is gaining increasing appeal for medical applications because antibiotic-resistant bacterial strains have become a major issue in public health care.[1−3] Silver-based medical products, ranging from topical ointments and bandages for wound healing to coated stents, have been proven to be effective in retarding and preventing bacterial infections.[4] Improvements in the development of novel silver nanoparticles-containing products are continuously sought. In particular, there is an increasing interest toward the exploitation of silver nanoparticles technology in the development of bioactive biomaterials, aiming at combining the relevant antibacterial properties of the metal with the peculiar performance of the biomaterial.[5−9]

However, a widely accepted consensus on the detailed molecular mechanism of silver nanoparticles toxicity is still missing. It is possible to state that a lack of physical barriers to nanoparticle diffusion into cells determines their generalized (bio)availability, with the risk of a massive uptake by eukaryotic cells, which eventually leads to their death.[10] A critical survey of the present nanotechnology literature suggests that the drive toward new formulations often overwhelms the interest for a better assessment of the cytotoxicity of the nanoparticles. In fact, the issue of possible adverse effects and toxicity of nanoparticles for the human body is progressively recognized as central by a still limited, albeit increasing, number of studies.[11] So far, water-based biomaterials able to successfully combine antibacterial properties of silver nanoparticles with demonstrated absence of cytotoxicity have not yet been reported in the literature. At the nanometric level, a crucial issue about silver nanoparticles is their tendency to aggregate, thus losing the peculiar properties associated with the nanoscale. Consequently, the preparation and stabilization of metal nanoparticles represent to date an open challenge. To this scope, polyelectrolytes in small concentration, such as polyphosphate, polyacrylate, poly(vinyl-sulfate), poly(ethylene-imine),[12−14] poly(allylamine),[8] and chitosan,[7,15,16] have been used with variable results to stabilize the nanoparticles preventing the growth of aggregates, in addition to the more widely used poly(vinylpyrrolidone),[17] a neutral polymer. The stabilization of metal nanoparticles is explained by the electronic interaction of the polymer functional groups with the metal particles. In fact, their (albeit minor) nucleophilic character is sufficient to bind the metal particles by donating electrons.[14] Protective polymers can coordinate metal ions before reduction, forming a polymer−metal ion complex; such a complex can then be reduced under mild conditions, resulting in a smaller size and a narrower size distribution than those obtained without protective polymers.[18] Once the reduction occurred, the stabilizing effect of these macromolecules is attributable to the fact that either the particles are attached to the much larger protecting polymers or the protecting molecules cover or encapsulate the metal particles.[8] To find applications in the biomaterials field, both the stabilizing and the reducing agents must not represent a biological hazard.[19]

Chitosan, a natural saccharidic polybase composed of β-(1→4)-linked glucosamine residues interspersed with residual *N*-acetylglucosamine moieties, has been previously used to prepare and stabilize metal nanoparticles.[7,15,16] However, the limitations of such polysaccharide are connected with its pH-dependent solubility (limited to low pH only, as a polycation), immiscibility with other oppositely charged polyelectrolytes and lack of cell-specific molecular signals. To overcome these problems, we decided to use a lactose-substituted chitosan, 1-deoxylactit-1-yl chitosan, short-named "Chitlac". Chitlac is a highly branched polymer devoid of pH limitations as to aqueous solubility; it is both biocompatible and bioactive, owing to the terminal galactose unit on the side chain.[20] In addition, at neutral pH the moderately cationic Chitlac can give rise to soluble binary mixtures with alginate, an anionic polysaccharide composed of (1→4)-linked α-L-guluronic acid and β-D-mannuronic acid

* To whom correspondence should be addressed. Tel.: +39 040 558 3682. Fax: +39 040 558 3691. E-mail: atravan@units.it.

10.1021/bm900039x CCC: $40.75
Published on Web 04/30/2009

residues. These mixtures were shown to be able to form stable hydrogels in cell-friendly conditions.[21,22]

The aim of this work is (i) to characterize the formation and stabilization of silver nanoparticles in Chitlac solutions, (ii) to assess the antimicrobial properties, either in solution or in 3D hydrogel structures, obtained by mixtures with the polysaccharide alginate, and (iii) to evaluate the cytotoxicity of the latter nanocomposite materials on different eukaryotic cell lines.

2. Materials and Methods

2.1. Materials. Chitlac (1-deoxylactit-1-yl chitosan, CAS registry number 85941-43-1) sample was prepared according to the procedure reported elsewhere[23] starting from a highly deacetylated chitosan (residual acetylation degree = 11.3%, Aldrich Chemical Co. (U.S.A.)). The molecular weight of Chitlac was estimated to be approximately 1.5×10^6. Alginate ($M_w \sim 130000$, $F_G = 0.65$, $F_{GG} = 0.53$) was provided by FMC Biopolymers. Silver nitrate, ascorbic acid, lead citrate, uranyl acetate, 4-(2-hydroxyethyl)-1-piperazine-ethanesulfonic acid, $CaCO_3$ (mean particle size 3 μm), glucono-D-lactone (GDL), and LDH (lactate dehydrogenase)-based TOX-7 kit (Sigma-Aldrich) were purchased from Sigma Chemical Co (St. Louis, MO). Mueller Hinton (MH) was from Difco Microbiology (Sparks, MD).

2.2. Chitlac−Silver Nanoparticles (Chitlac-nAg) Preparation. Silver nanoparticles were obtained by reducing silver ions with ascorbic acid in Chitlac solutions according to the following procedures: freeze-dried Chitlac was dissolved in deionized water to obtain solutions with different concentrations (1, 2, and 4 g/L). Chitlac solutions were mixed with $AgNO_3$ solutions to achieve final $AgNO_3$ concentrations of 0.5 and 1 mM; then ascorbic acid ($C_6H_8O_6$) solutions were added at final concentrations of 0.25 and 0.5 mM, respectively. For antibacterial tests 20% Mueller−Hinton broth was added to Chitlac-nAg solutions.

2.3. Hydrogels Preparation. *2.3.1. AC-Gel.* For the preparation of alginate−Chitlac hydrogels (AC-Gel), an in situ calcium release approach was used. Briefly, a Chitlac solution was added to an alginate solution (final concentrations: alginate 15 g/L, Chitlac 2 g/L, NaCl 0.15 M, HEPES buffer 0.01 M, pH 7.4) and the mixture was blended with an inactivated form of Ca^{2+} ($CaCO_3$, 15 mM) followed by the addition of the slowly hydrolyzing D-glucono-δ-lactone (GDL; $[GDL]/[Ca^{2+}] = 2$). Aliquots of this gelling solution were poured into well tissue culture plates. Finally, the gels were washed with $CaCl_2$ solution 5 mM to remove residual GDL. For antibacterial tests, 20% Mueller−Hinton broth was added to both Chitlac and alginate solutions.

2.3.2. AC-nAg-Gel. Alginate−Chitlac hydrogels containing silver nanoparticles were prepared according to the procedure of the AC-Gels using Chitlac-nAg instead of Chitlac solutions. For antibacterial tests, 20% Mueller−Hinton broth was added to both Chitlac and alginate solutions.

2.4. UV−Vis Spectroscopy. UV−visible spectroscopy measurements were performed with a Cary 400 spectrophotometer (data interval, 0.5 nm; scan speed, 300 nm/min). All samples solutions were diluted 1:10.

2.5. Transmission Electron Microscopy (TEM). TEM images were taken by means of a PHILIPS EM 208 Microscope; the solutions were deposited onto Nickel grids coated with a carbon film and dried overnight. In the samples in which the polymer was stained, a mixed solution of lead citrate (5 g/L) and uranyl acetate (5 g/L) was added 1:1 to the Chitlac−silver nanoparticles (nAg) solutions.

2.6. Bacterial Killing Kinetics Assays. The killing kinetics assays were performed using cultures of *E. coli* (ATCC 25922), *S. epidermidis* (clinical isolate), *S. aureus* (ATCC 25923), and *P. aeruginosa* (ATCC 27853) diluted in 20% Mueller−Hinton broth to give 1×10^6 CFU/mL (CFU = colony forming units) in the presence or absence of Chitlac-nAg. The bacterial suspensions were then incubated in a shaking water bath at 37 °C. At the indicated times, samples were removed, serially diluted with buffered saline solution, plated in duplicate on Mueller−Hinton agar, and incubated for 24 h to allow colony counts. Data are the mean of at least four independent determinations with comparable results.

2.7. Growth Inhibition Assays in Solid Medium. The growth inhibition in solid medium was evaluated after smearing, with sterile cotton swabs, of bacterial suspensions at final concentrations of 10^6 and 10^5 CFU/mL on Petri dishes prepared as described above (hydrogel preparation). After overnight incubation at 37 °C, the presence of visible colonies was evaluated. Growth controls were carried out on Mueller−Hinton agar plates and AC gels in the presence of Mueller−Hinton medium.

2.8. Evaluation of Bacterial Membrane Alteration by Flow Cytometric Assays. Flow cytometric assays were used to evaluate the transmembrane potential and the membrane permeabilization of bacterial cells treated with the system Chitlac-nAg. For these analyses, midlogarithmic phase bacterial cultures were diluted in 20% MH broth to 1×10^6 CFU/mL. Aliquots of the bacterial suspension were then incubated with or without (controls) the system Chitlac-nAg for 10 or 30 min at 37 °C. At the end of the incubation time, the bacterial suspensions were incubated in the dark for 4 min at 37 °C with bis-(1,3-dibutylbarbituric acid)-trimethine oxonol ($DiBAC_4(3)$; Molecular Probes Inc., Eugene, OR) at a final concentration of 1 μM to evaluate alterations in the transmembrane potential. The fluorescence intensity was detected with a Cytomics FC 500 instrument (Beckman-Coulter, Inc., Fullerton, CA) equipped with an argon laser (488 nm, 5 mW) and using a photomultiplier tube fluorescence detector for green (525 nm) filtered light. The detectors were set on logarithmic amplification. Optical and electronic noise were eliminated by setting an electronic gating threshold on forward scattering detector, while the flow rate was kept at a data rate below 200 events/second to avoid cell coincidence. For each sample, at least 10000 events were acquired and stored as list mode files. Membrane permeabilization following treatment with the system Chitlac-nAg was determined by means of a flow cytometer, measuring the propidium iodide (PI; Sigma-Aldrich) uptake by bacterial cells. For the analyses, bacterial suspensions of 1×10^6 cells/mL were incubated in 20% MH broth with the system Chitlac-nAg at 37 °C for different times. A filtered solution of propidium iodide was then added to the bacterial suspensions at a final concentration of 10 μg/mL, and the cells were analyzed in the flow cytometer after 4 min incubation at 37 °C. The fluorescence intensity was detected as reported above using a detector for red light (610 nm). All the experiments with the fluorescent probes were conducted in triplicate and the analysis of data was performed with the WinMDI software (Dr. J. Trotter, Scripps Research Institute, La Jolla, CA, U.S.A.).

2.9. LDH Cytotoxicity Assay. In vitro cytotoxicity of AC-nAg-Gels was evaluated by using the lactate dehydrogenase assay (LDH assay, TOX-7, Sigma) on the mouse fibroblast-like (NIH-3T3), human hepatocarcinoma (HepG2), and human osteosarcoma (MG63) cell lines, respectively. Cylindrical gel samples, with a length of 5 mm and a diameter of 4 mm, were used and the tests were performed by direct contact with the gel or with liquid extract of the gel material. For a direct contact test, 70000 cells were plated on 24-well plates and, after complete adhesion, culture medium was changed with 250 μL of fresh medium. Tested materials (in quadruplicate) were directly deposited on the cell layer. After 24 and 72 h, medium was collected and the LDH assay was performed according to the manufacture's protocol. In an extraction test, samples were incubated in extraction medium (Dulbecco's modified Eagle's medium, inactivated fetal bovine serum 10%, penicillin 100 U/mL, streptomycin 100 μg/mL, and L-glutamine 2 mM) for 24 h at 37 °C and 5% pCO_2. The surface/volume ratio of the samples and the medium was 1.25 cm^2/mL. After incubation, extraction media were added on cells seeded on 24-well plates (70000 cells/well). The LDH assays were performed after 24 and 72 h as described above. Each material test was performed in quadruplicate. Evaluation of cytotoxicity was calculated according to the formula: % LDH released = $[(A - B)/(C - B)] \times 100\%$, with A = LDH activity in the culture medium of gel-treated or extraction medium-treated cells; B = LDH activity of culture medium from untreated cells; and C = LDH activity after total cell lysis).

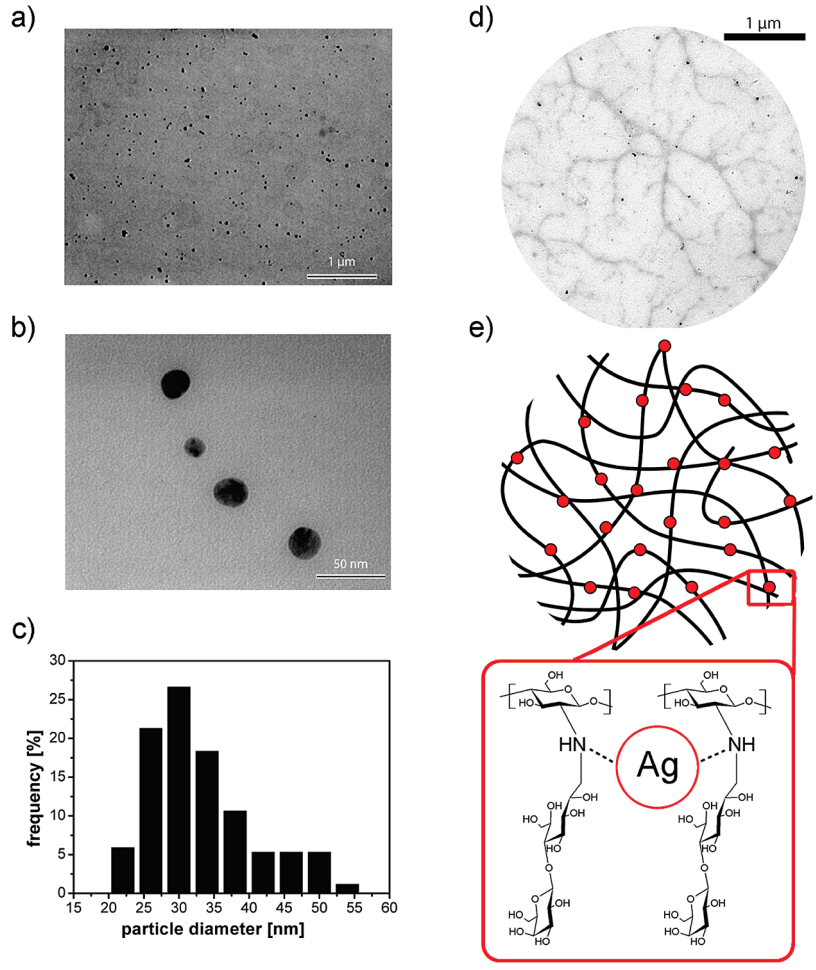

Figure 1. (a,b) TEM images of silver nanoparticles dispersed in Chitlac at different magnifications (Chitlac 4 g/L, $AgNO_3$ 1 mM, $C_6H_8O_6$ 0.5 mM); (c) silver nanoparticles size distribution histogram based on the TEM image in Figure 1a; the mean particle size is 33.6 ± 7.6 nm; (d) TEM image of silver nanoparticles formed on the polymeric chains of Chitlac (Chitlac 2 g/L, $AgNO_3$ 1 mM, $C_6H_8O_6$ 0.5 mM). Chitlac chains have been stained with a mixed solution of lead citrate (5 g/L) and uranyl acetate (5 g/L); (e) schematic representation of the polymeric chains of Chitlac providing the nitrogen atoms for the coordination and stabilization of silver nanoparticles.

2.10. Preparation of Microspheres and ICP-MS Analysis. Calcium microspheres from AC-nAg mixtures (final concentrations: alginate 15 g/L, Chitlac 2 g/L nAg, NaCl 0.15 M, HEPES 0.01 M, pH 7.4) were obtained by dripping the polymer blend into a gelling solution (0.05 M $CaCl_2$). The droplet size was controlled by use of a high-voltage electrostatic bead generator (7 kV, 10 mL/h, steel needle with 0.7 mm outer diameter, 1 cm distance from the needle to the gelling solution). The gel beads obtained were stirred for 30 min in the gelling solution prior to use.

To evaluate the amount of silver released from the AC-nAg gel, the microspheres were vigorously stirred for 5 weeks in a saline solution (NaCl 0.015 M) with a volume ratio microspheres/solution of 4; after incubation, supernatants from the microsphere suspensions were analyzed by ICP-MS (inductively coupled plasma mass spectrometry).

2.11. MTT Assay. Cytotoxicity of AC-nAg gel microspheres external solutions was evaluated by the MTT (3-(4,5-dimethylthiazol-2-yl)-2,5-diphenyltetrazolium bromide) reduction assay using mouse fibroblast (NIH-3T3), human hepatocarcinoma (HepG2), and human osteosarcoma (MG63) cell lines, respectively. Cells (5000 cells/well) were seeded into 96-well plates and allowed to adhere for 16 h. Extracts from the microspheres were then added to cell cultures for 72 h at 37 °C in the presence of DMEM culture medium and 10% fetal bovine serum. Cell cultures treated with 1% (v/v) Triton-X 100 in complete DMEM medium or with a solution of 0.015 M NaCl supplemented with DMEM culture medium and fetal bovine serum were used, respectively, as positive and negative controls. Finally, MTT (5 mg/mL in PBS) was added to the medium in each well to obtain a final concentration of 0.5 mg/mL, and the cell cultures were incubated for a further 4 h. Cell viability was determined by measuring the cellular reduction of MTT to the crystalline formazan product, which was dissolved by addition of 100 μL of DMSO. The formazan concentration was determined spectrophotometrically at 570 nm.

3. Results and Discussion

Chitlac nanocomposites containing silver were prepared by chemical reduction of corresponding metal ions to zeroth-valent metal nanoparticles; the reduction was performed using ascorbic acid, a nontoxic reagent which can form metallic silver according to the following stoichiometry:[6]

$$2Ag^+ + C_6H_8O_6 \rightleftarrows 2Ag^0 + C_6H_6O_6 + 2H^+$$

The formation of nanoparticles, their shape, distribution and dimensions have been evaluated by means of transmission electron microscopy (TEM) imaging and analyses. Figure 1a,b shows the nanoparticles dispersed in Chitlac at two different magnifications; they are mostly round-shaped and well-dispersed. TEM images have been analyzed to evaluate the dimensional distribution, as the size affects the antimicrobial properties of the nanoparticles.[24] The histogram shows a narrow distribution of the silver nanoparticles dispersed in Chitlac with a maximum frequency at around 30 nm (Figure 1c) and a mean

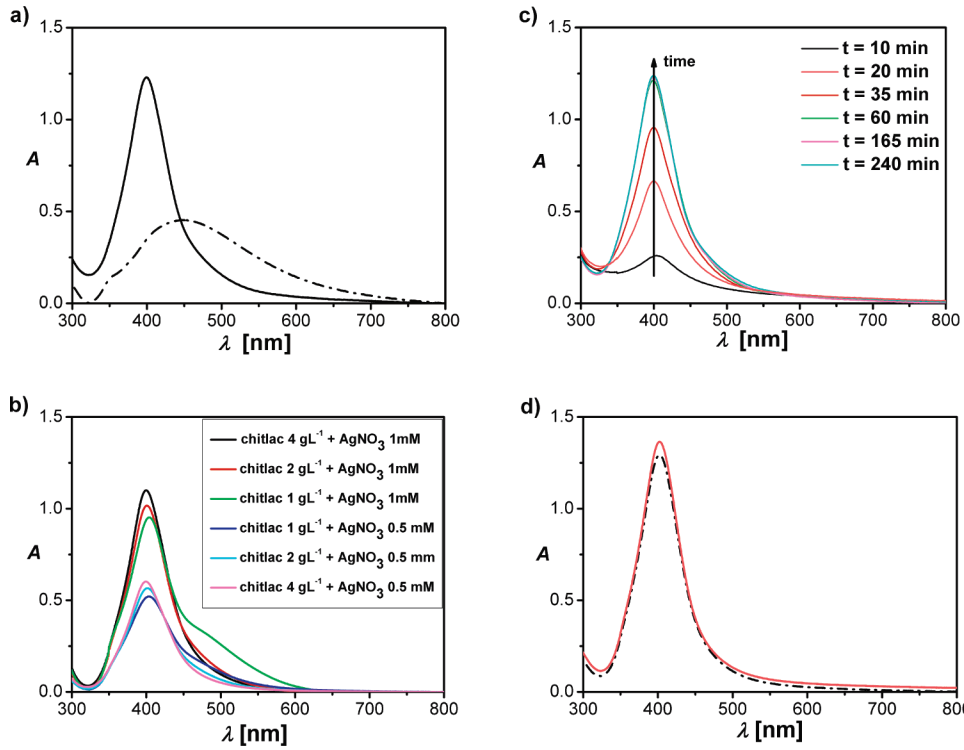

Figure 2. (a) UV−vis spectra of silver nanoparticles formed in chitosan (dashed line) and Chitlac (solid line) solutions under the same conditions (polymer concentrations 2 g/L; $AgNO_3$ 1 mM; $C_6H_8O_6$ 0.5 mM). (b) Effect of polymer and $AgNO_3$ concentrations on UV−vis spectra of silver nanoparticles. In each sample, the $AgNO_3/C_6H_8O_6$ concentration ratio is 2, according to the reaction stoichiometry. (c) Time dependence of UV−vis spectra variations of Chitlac 2 g/L + $AgNO_3$ 1 mM after the addition of ascorbic acid. d) UV−vis spectra of silver nanoparticles in Chitlac after 1 day (black dashed line) and after 90 days (orange solid line).

diameter of 33.6 ± 7.6 nm. TEM analyses were conducted also to visualize the polymeric chains using staining agents (i.e., Pb^{2+}, UO_2^{2+}). As revealed by Figure 1d, Chitlac chains ("gray threads") efficiently coordinate the silver nanoparticles ("black dots"), thus hampering their large scale collapsing (Figure 1e); the image shows a vein-like structure formed by different polysaccharide chains, which likely associate as a consequence of the drying process during sample preparation for TEM analysis.

The formation of silver nanoparticles was verified also by means of UV−vis absorption spectroscopy (Figure 2a), where an intense band centered at about 400 nm was clearly detected. This band, identified as a "surface plasmon resonance band", is due to a collective excitation of the free electrons in the nanoparticles. The shape of the plasmon band is almost symmetrical, suggesting that the nanoparticles are well dispersed and spherical. At variance, the aggregation of nanoparticles would lead to a broader plasmon band, with a red-shifted maximum.

The effect of concentration in solution of both polymer and silver nitrate was explored (Figure 2b). The changes in UV−vis absorption indicate that the size and dispersion of silver nanoparticles were affected by both the concentration of Chitlac (which operates as a controller of nucleation as well as a stabilizer) and of $AgNO_3$. The highest plasmon peaks were recorded for Chitlac at 2 and 4 g/L in the presence of $AgNO_3$ 1 mM and $C_6H_8O_6$ 0.5 mM. The kinetics of the reduction process was monitored for 4 h immediately after the addition of ascorbic acid (Figure 2c). It can be seen that the intensity of the plasmon resonance peak increases with time; for reaction times exceeding 4 h no significant increase in the absorption peak was found. As previously noted, long-term stability of silver nanoparticles in solution is an important goal to be reached. In fact, agglomeration of particles may occur upon aging of solutions which initially contained isolated particles. Figure 2d shows that the presence of Chitlac allows the stabilization of silver nanoparticles in solution up to several months, thus preventing colloidal instability. In view of this result, it can be safely stated that Chitlac acts as an efficient stabilizing ligand for silver ions and silver nanoparticles thanks to the presence of amino groups. Esumi[18] demonstrated that metal nanoparticles can be protected by the exterior amino groups of dendrimers which act as stabilizers. When $AgNO_3$ is mixed with Chitlac solutions, Ag^+ ions probably give rise to a localized binding to Chitlac macromolecules via amino groups chelation persisting also with the formed silver nanoparticles.

The hydrophilic side-chains also play a fundamental role in the stabilization by embedding the silver nanoparticles bound in the proximity of the polymer backbone and isolating them from the surrounding species (Figure 1e). In fact, it is known that chitosan, which shares with Chitlac the same backbone chemical structure, is able to stabilize silver nanoparticles according to the same mechanism proposed above. However, a comparison of the UV−vis spectra arising from the reduction of silver ions in the presence of Chitlac or chitosan points to a marked difference in behavior of the two polysaccharides under the same experimental conditions (Figure 2a). In fact, a broader, less intense and nonsymmetrical peak was detected for chitosan, suggesting the formation of more aggregated nanoparticles. The better performance of Chitlac must be traced back to the presence of the highly hydrophilic and bulky lactitol groups decorating the modified polysaccharide; they provide silver nanoparticles with coordination (amino groups) and protection (steric hindrance), thus preventing their aggregation.

In order to study the antimicrobial activity of Chitlac-nAg, killing kinetics assays were performed with *S. epidermidis*, *E.*

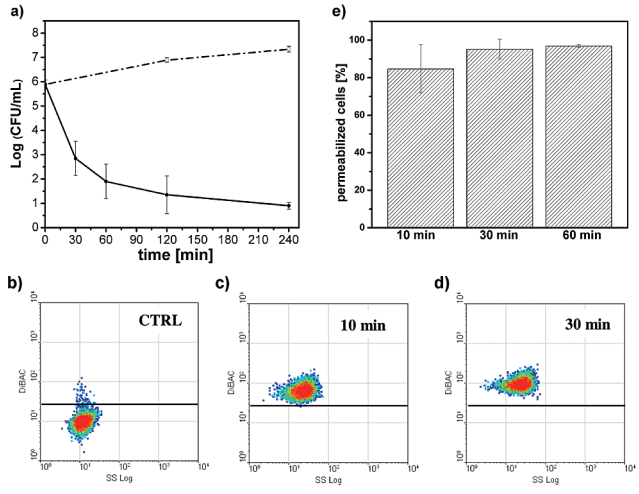

	Depolarized Cells [%]	MFI
Control 10 min	2.5±0.8	8.2±1.8
Chitlac-nAg 10 min	97.5±3.9	57.1±6.0
Control 30 min	8.8±5.0	11.0±3.8
Chitlac-nAg 30 min	99.6±0.4	81.7±13.3

Figure 3. (a) Killing kinetics of Chitlac-nAg (solid line) against *S. epidermidis*. The dashed line indicates control runs in the absence of Chitlac-nAg. Results are mean values (±SD) of at least four independent determinations; (b−d) Dual-parameter dot plot of the side scatter intensity versus DiBAC4(3) fluorescence relative to *S. epidermidis* after incubation with Chitlac-nAg; (b) CTRL = control at 10 min, (c) Chitlac-nAg treated sample after 10 min, (d) Chitlac-nAg treated sample after 30 min. The table reports the percentage of depolarized cells and the corresponding mean fluorescence intensity (MFI) values in nontreated and Chitlac-nAg treated samples; (e) effect of Chitlac-nAg on the membrane integrity of *S. epidermidis*. Bacteria were incubated for 10, 30, and 60 min with Chitlac-nAg in 20% MH broth. The percentage of PI-fluorescent cells after treatment is shown. Background values obtained with untreated samples (<5% of permeabilized cells) were subtracted to each nAg-treated sample. Results are the mean (±SD) of 3 independent experiments.

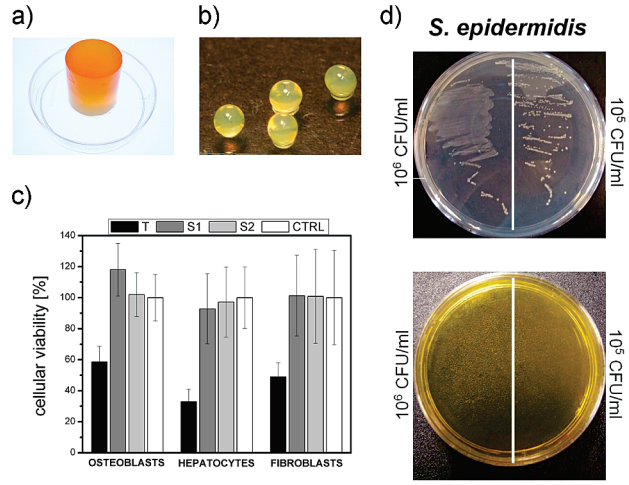

Figure 4. (a) Mixed alginate−Chitlac cylindrical hydrogel containing silver nanoparticles (AC-nAg gel). (b) AC-nAg microspheres. (c) Cytotoxicity analysis (MTT assay) on mouse fibroblast (NIH-3T3), human hepatocarcinoma (HepG2), and human osteosarcoma (MG63) cell lines of AC-nAg gel microspheres external solutions (S1 and S2, external solutions not diluted and 1:10 diluted, respectively; T, cytotoxicity positive control, cells treated with Triton 1%; CTRL, cytotoxicity negative control, cells treated with 0.015 M NaCl solution). (d) Growth of *S. epidermidis* on 20% Mueller−Hinton AC gel (upper Petri dish) and on 20% Mueller−Hinton AC-nAg gel (lower Petri dish).

coli, *S. aureus*, and *P. aeruginosa* to determine the amount of viable cells after treatment with Chitlac-nAg solutions. Bacteria were incubated with Chitlac-nAg for different times and then plated on Mueller−Hinton agar to allow counting of colony forming units (CFU). Overall, the Chitlac-nAg system showed a remarkable bactericidal effect against all four bacterial strains with a very fast killing kinetics: as representative data, Figure 3a reports the results for the *S. epidermidis* strain. The number of viable cells drastically decreased (a drop of 3 log units in CFU/mL) after only 30 min of incubation with the Chitlac-nAg system and, after 2 h of treatment, a complete inactivation of bacterial cells was found.

To study the mechanism by which the system Chitlac-nAg inactivates bacterial cells, the effect on membrane potential was evaluated by flow cytometry. Cell membrane depolarization was assessed by addition of DiBAC4(3), a fluorescent probe able to selectively enter and fluorescently label the cells whose membrane potential has collapsed, resulting in an increase of the mean fluorescence intensity (MFI). The fluorescence intensity of *S. epidermidis* was shifted toward higher channel numbers with respect to untreated cells after only 10 min of incubation with the system Chitlac-nAg, revealing a remarkable depolarization of the cell population (97.5 ± 3.9% of fluorescent cells vs 2.5 ± 0.8% of the control; Figure 3b−d).

The depolarization effect shown by the use of the DiBAC4(3) probe suggests that the system Chitlac-nAg interacts with the bacterial membranes. To evaluate the membrane damage caused by the system Chitlac-nAg, untreated and treated bacterial cells were labeled with the fluorescent probe propidium iodide (PI), which is excluded from cells with an intact plasma membrane and thus used as a marker of membrane integrity. A remarkable permeabilizing effect was observed after treatment of *S. epidermidis*; when the cells were incubated with Chitlac-nAg for 10 min, the percentage of PI-positive cells was of 80% versus <5% of the control. The membrane damage is even more evident after 30 and 60 min of treatment (>90% PI-positive cells; Figure 3e). Similar results of antibacterial activity were obtained with all the bacterial strains tested.

LDH tests carried out on the system Chitlac-nAg in solution pointed out a cytotoxic effect on mouse fibroblast (NIH-3T3), human hepatocarcinoma (HepG2), and human osteosarcoma (MG63) cell lines leading to cell death after 24 h (data not shown). This observation prompted us to focus our attention toward the preparation of Chitlac-based 3D structures entrapping the silver nanoparticles. If successful, such hydrogels could possibly be used in the preparation of bioactive biomaterials. To this end, the gel forming properties of alginate were exploited allowing the production of a highly hydrated system in a mixture with Chitlac-nAg. The rationale of this approach is that the 3D system could prevent nanoparticles from being available for eukaryotic cellular uptake but, at the same time, preserve its antimicrobial activity allowing the direct interaction of the nanoparticles with the proteins localized on the bacterial surface. In fact, in bacteria the thiol groups (-SH) of membrane proteins, exposed to the extracellular portion of the membrane, are the main molecular targets of the silver antibacterial activity.[25−29] At variance, eukaryotic cells do not have exterior thiol groups, thus silver ions or nanoparticles must first permeate through cell membranes to react with -SH groups of intracellular proteins and enzymes, such as inner membrane mitochondrial proteins and the enzymes of the antioxidant defense mechanism.[30−36] The use of alginate allows casting of different gel shapes (cylinders, slabs, microcapsules, etc.), which makes it possible to tailor-make different semisolid systems for various applications. The advantage of the presence of Chitlac over chitosan

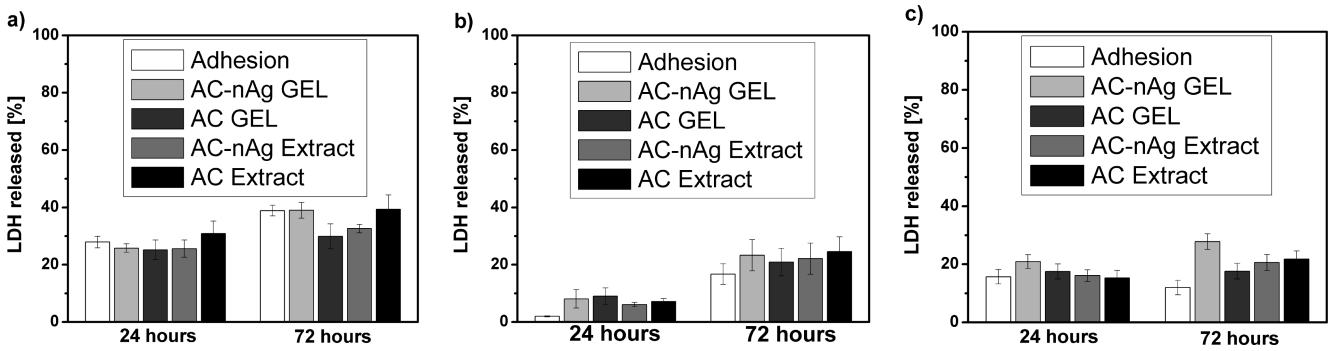

Figure 5. Effect of AC-nAg gels on LDH leakage from (a) mouse fibroblast (NIH-3T3), (b) human hepatocarcinoma (HepG2), and (c) human osteosarcoma (MG63) cell lines. The cytotoxicity test was performed both with the extract from gel material (AC-nAg extract) and with the gel material itself by direct contact with cell layer (AC-nAg GEL). Control cells cultured in adhesion in complete DMEM medium and cells treated with AC gels lacking silver nanoparticles (AC GEL and AC extract) were run in parallel to AC-nAg gels treated groups. The percentage of LDH release was calculated by dividing the amount of activity in the medium by the total activity (medium and cell lysate) after subtraction of the control. The data are expressed as mean ± SD of four independent experiments.

in the preparation of three-dimensional gels is connected with the ability of the former to allow complete miscibility between the two oppositely charged biopolymers, as already pointed out,[21] at variance with the latter polycation. This process can thus be efficiently exploited to entrap silver nanoparticles stabilized by polycations within a homogeneous gel construct avoiding coacervation. The final nanocomposite structure arising from the treatment of the binary mixture of alginate and Chitlac-nAg with calcium was a yellow-orange yet transparent hydrogel. (Figure 4a). It is important to underline that neither nanoparticles aggregation nor polymer phase separation was observed during and after gel formation. Homogeneous highly swollen microspheres (Ø = 500 μm) were obtained[37] (Figure 4b), which ensure a high surface/volume ratio. The amount of silver released by AC-nAg gel microspheres[0] was evaluated from two independent measurements. The microspheres were kept under vigorous stirring for 5 weeks in saline solution with a microspheres/solution volume-ratio of 4; the external solution was eventually analyzed by ICP-MS to evaluate the amount of silver released by the microspheres. The concentration of silver released was 58 μg/L, which corresponds to 2.6% of the total silver amount inside the microspheres, pointing out that a very low amount of silver had been released from the gel. The MTT tests showed that such low concentration of silver released from the microspheres was not cytotoxic for three different cell lines: fibroblasts (NIH-3T3), osteoblasts (MG63), and hepatocytes (HepG2; Figure 4c).

The possibility of obtaining three-dimensional highly hydrated structures results particularly appealing for tissue engineering applications in which an ideal candidate biomaterial must associate antibacterial properties with lack of cytotoxicity. To assess the extent of bacterial growth on semisolid system, two different concentrations of the four bacterial strains (10^6 and 10^5 CFU/mL, respectively) were smeared on the surface of nanocomposite AC-nAg gel. Both agar and alginate−Chitlac gels (AC gels) were used as controls. After overnight incubation, bacterial colonies were clearly visible on control plates, while they were completely absent on the silver nanoparticles-containing gels. Figure 4d shows the case of *S. epidermidis*; similar results were obtained with all the strains tested (data not reported).

We evaluated the cytotoxicity of the nanocomposite system also in the form of gel (AC-nAg). As reported in Figure 5, AC-nAg gels did not exert any cytotoxic effect on the cell lines used. In fact, there was no significant difference in the release of lactate dehydrogenase between the AC-nAg treated cells and control groups after 24 and 72 h.

The combination of these results shows that the AC-nAg hydrogels, besides providing for an efficient stabilization of the silver nanoparticles against aggregation, are able to display antibacterial activity without being harmful to mammalian cells. In the AC-nAg gels, nanoparticles coordinated to Chitlac are firmly grafted and immobilized in the gel matrix and therefore do not diffuse into the surrounding environment, as demonstrated by the ICP-MS analysis.

4. Conclusions

In this work we have successfully obtained new nanocomposite systems based on polysaccharides and silver nanoparticles. The role of the branched polysaccharide Chitlac is fundamental in the formation and stabilization of well-dispersed silver nanoparticles having a mean diameter of about 35 nm. Reproducibility of size distribution together with a demonstrated stability of the nanoparticles over time have been successfully achieved. Moreover, the use of a nondemanding chemical approach adds a considerable appeal to the results obtained. The simultaneous presence, in the final system, of a sugar-based bioactive polymer for cell stimulation[22] and of silver nanoparticles for antibacterial activity represents a major achievement of the present work. This novel approach arises at the crossover of nanotechnology and glycobiology. It might pave the way (i) to facilitate the use of silver nanoparticle-biopolymer composites in the preparation of bioactive biomaterials and (ii) to provide new tools to design engineered materials exploiting, to different purposes, the bioactivity provided by the carbohydrate component and the properties of silver at the nanoscale level.

Acknowledgment. The authors would like to acknowledge Prof. G. Adami for the ICP-MS measurements. This study was supported by grants from the Italian Ministry for University and Research (PRIN 2007), the Friuli Venezia Giulia Region (LR 26/2005, art. 23 for the R3A2 network), and the EU-FP6 Project "NEWBONE" (Contract Number 026279-2).

References and Notes

(1) Chastre, J. *Clin. Microbiol. Infect.* **2008**, *14* (Suppl 3), 3–14.
(2) Slama, T. G. *Crit. Care* **2008**, *12* (Suppl 4), S4.
(3) Goldmann, D. A.; Weinstein, R. A.; Wenzel, R. P.; Tablan, O. C.; Duma, R. J.; Gaynes, R. P.; Schlosser, J.; Martone, W. J. *JAMA, J. Am. Med. Assoc.* **1996**, *275* (3), 234–240.
(4) Chen, J. P. *J. Invasive Cardiol.* **2007**, *19* (9), 395–400.
(5) Balogh, L.; Swanson, D. R.; Tomalia, D. A.; Hagnauer, G. L.; McManus, A. T. *Nano Lett.* **2001**, *1* (1), 18–21.

(6) Fu, J.; Ji, J.; Fan, D.; Shen, J. *J. Biomed. Mater. Res., Part A* **2006**, *79* (3), 665–674.
(7) Huang, H.; Yuan, Q.; Yang, X. *Colloids Surf., B* **2004**, *39* (1−2), 31–37.
(8) Kuo, P. L.; Chen, W. F. *J. Phys. Chem. B* **2003**, *107* (41), 11267–11272.
(9) Sanpui, P.; Murugadoss, A.; Prasad, P. V. D.; Ghosh, S. S.; Chattopadhyay, A. *Int. J. Food Microbiol.* **2008**, *124* (2), 142–146.
(10) Geiser, M.; Rothen-Rutishauser, B.; Kapp, N.; Schurch, S.; Kreyling, W.; Schulz, H.; Semmler, M.; Im, H., V.; Heyder, J.; Gehr, P. *Environ. Health Perspect.* **2005**, *113* (11), 1555–1560.
(11) Chen, X.; Schluesener, H. J. *Toxicol. Lett.* **2008**, *176* (1), 1–12.
(12) Dai, J. H.; Bruening, M. L. *Nano Lett.* **2002**, *2* (5), 497–501.
(13) Grunlan, J. C.; Choi, J. K.; Lin, A. *Biomacromolecules* **2005**, *6* (2), 1149–1153.
(14) Henglein, A. *J. Phys. Chem.* **1993**, *97* (21), 5457–5471.
(15) dos Santos, D. S.; Goulet, P. J. G.; Pieczonka, N. P. W.; Oliveira, O. N.; Aroca, R. F. *Langmuir* **2004**, *20* (23), 10273–10277.
(16) Yi, Y.; Wang, Y.; Liu, H. *Carbohydr. Polym.* **2003**, *53* (4), 425–430.
(17) Yu, H.; Xu, X.; Chen, X.; Lu, T.; Zhang, P.; Jing, X. *J. Appl. Polym. Sci.* **2006**, *103*, 125−133.
(18) Esumi, K.; Suzuki, A.; Aihara, N.; Usui, K.; Torigoe, K. *Langmuir* **1998**, *14* (12), 3157–3159.
(19) Huang, H.; Yang, X. *Carbohydr. Res.* **2004**, *339* (15), 2627–2631.
(20) Donati, I.; Stredanska, S.; Silvestrini, G.; Vetere, A.; Marcon, P.; Marsich, E.; Mozetic, P.; Gamini, A.; Paoletti, S.; Vittur, F. *Biomaterials* **2005**, *26* (9), 987–998.
(21) Donati, I.; Haug, I. J.; Scarpa, T.; Borgogna, M.; Draget, K. I.; Skjåk-Bræk, G.; Paoletti, S. *Biomacromolecules* **2007**, *8* (3), 957–962.
(22) Marsich, E.; Borgogna, M.; Donati, I.; Mozetic, P.; Strand, B. L.; Salvador, S. G.; Vittur, F.; Paoletti, S. *J. Biomed. Mater. Res., Part A* **2007**, *84* (2), 364−376.
(23) Yalpani, M.; Hall, L. D. *Macromolecules* **1984**, *17* (3), 272–281.
(24) Panacek, A.; Kvitek, L.; Prucek, R.; Kolar, M.; Vecerova, R.; Pizurova, N.; Sharma, V. K.; Nevecna, T.; Zboril, R. *J. Phys. Chem. B* **2006**, *110* (33), 16248–16253.
(25) Clement, J. L.; Jarrett, P. S. *Met. Based Drugs* **1994**, *1* (5−6), 467–482.
(26) Feng, Q. L.; Wu, J.; Chen, G. Q.; Cui, F. Z.; Kim, T. N.; Kim, J. O. *J Biomed. Mater. Res.* **2000**, *52* (4), 662–668.
(27) Elechiguerra, J.; Burt, J.; Morones, J.; Camacho-Bragado, A.; Gao, X.; Lara, H.; Yacaman, M. *J. Nanobiotechnol.* **2005**, *3* (1), 6.
(28) Morones, J. R.; Elechiguerra, J. L.; Camacho, A.; Holt, K.; Kouri, J. B.; Ramirez, J. T.; Yacaman, M. J. *Nanotechnology* **2005**, *16* (10), 2346–2353.
(29) Nel, A. *Science* **2005**, *308* (5723), 804–806.
(30) Braydich-Stolle, L.; Hussain, S.; Schlager, J. J.; Hofmann, M. C. *Toxicol. Sci.* **2005**, *88* (2), 412–419.
(31) Hussain, S. M.; Hess, K. L.; Gearhart, J. M.; Geiss, K. T.; Schlager, J. J. *Toxicol. In Vitro* **2005**, *19* (7), 975–983.
(32) Hussain, S. M.; Javorina, A. K.; Schrand, A. M.; Duhart, H. M.; Ali, S. F.; Schlager, J. J. *Toxicol. Sci.* **2006**, *92* (2), 456–463.
(33) Kone, B. C.; Kaleta, M.; Gullans, S. R. *J. Membr. Biol.* **1988**, *102* (1), 11–19.
(34) Oberdorster, G.; Maynard, A.; Donaldson, K.; Castranova, V.; Fitzpatrick, J.; Ausman, K.; Carter, J.; Karn, B.; Kreyling, W.; Lai, D.; Olin, S.; Monteiro-Riviere, N.; Warheit, D.; Yang, H.; ILSI Research Foundation, A. r. f. t. *Part. Fibre Toxicol.* **2005**, *2* (1), 8.
(35) Donaldson, K.; Tran, C. L. *Inhalation Toxicol.* **2002**, *14* (1), 5–27.
(36) Donaldson, K.; Stone, V.; Tran, C. L.; Kreyling, W.; Borm, P. J. *Occup. Environ. Med.* **2004**, *61*, 727–728.
(37) Strand, B. L.; Gåserød, O.; Kulseng, B.; Espevik, T.; Skjåk-Bræk, G. *J. Microencapsulation* **2002**, *19* (5), 615–630.

BM900039X